Proceedings, Bicycle and Motorcycle Dynamics 2019
Symposium on the Dynamics and Control of Single Track Vehicles,
9–11 September 2019, University of Padova, Italy

Gyroscopic stabilisers for powered two-wheeled vehicles

R. Lot, J. Fleming

Mechanical Engineering Department
Faculty of Engineering and Physical Sciences
University of Southampton
University Road, SO17 1BJ, UK
e-mail: Roberto.Lot@soton.ac.uk, J.M.Fleming@soton.ac.uk

ABSTRACT

This paper illustrates the potential of an active gyroscopic stabiliser for the stabilisation of single track vehicles, at low and high speed as well as during braking. Alternative systems are considered, including single and twin counter-rotating gyroscopes, spinning and precessing with respect to different axes. The gyroscope system is actively controlled with an optima Linear Quadratic Regulator. A suitable mathematical model has been developed and stability has been investigated both by eigenvalue calculation and time domain simulations. We found that the most effective configuration is one where the gyroscope(s) spin with respect to an axis parallel to the wheels' spin axis and swing with respect to the vehicle yaw axis. Actively controlled gyroscopes are capable of stabilising the vehicle in its whole range of operating speed, as well as during braking. The alteration of the original vehicle handling characteristics is negligible when active counter-rotating gyroscopes are used, and still acceptable if a single gyroscope is adopted instead.

Keywords: motorcycles; single-track vehicles; stability; gyroscopic stabilisation; LQR control.

1 INTRODUCTION

It is well known that motorcycles and single track vehicles in general may suffer serious stability problems [20, 14, 5, 6]. More specifically, there are three typical modes that may become unstable depending on vehicle characteristics and motion conditions: capsize, weave, and wobble. The Capsize mode is stable at null and low speed and becomes mildly unstable after the minimum speed threshold has been passed. The Weave mode consists of oscillation of the whole vehicle at a frequency between 2 and 4 Hz, it is unstable at low speed, becoming stable as the speed increases but finally it may become unstable again at high speed. Finally, the Wobble mode mainly consists of the oscillation of the steering assembly, typically with a frequency between 5 and 9 Hz, and may become unstable in the medium speed range. Such stability problems are even more pronounced under acceleration and braking [14, 5], or while cornering [5].

Instability is certainly one of the reasons that collision avoidance systems, automated emergency braking, and other similar active safety technologies have not been developed yet for motorcycles, while they are already available for cars. There are at least two technologies that may be exploited for stabilisation and active safety of motorcycles: steer-by-wire and gyroscopic stabilisation. In a steer-by-wire system, the direct mechanical connection between the handlebars and the front wheel is replaced by an electro-mechanical system which actively controls the wheel steer angle. A discussion about this topic is out of scope of the present article, which focuses on gyroscopic stabilisation only, but some details may be found in [18]. Early references for gyroscopic stabilisers for automotive applications date back to the 19^{th} century [1], followed by similar patents at the beginning of the 20^{th} century. The stabilisation of the roll of motorcycle by the precession of a gyro rotor of high moment of inertia spinning at high speed is claimed by [22], similar ideas are proposed by [9] for a toy motorcycle application. In recent times, [12, 11, 13] claim the idea of using a couple of identical gyroscopes spinning and precessing in opposite directions, so a gyroscopic torque effect is generated only when the precession motion is activated Gyroscopes may also be used for regenerative braking [12, 11]. Despite this practical interest in the subject, the scientific literature on this topic is scarce and incomplete. In [2], a gyroscopic stabiliser consisting of two identical gyroscopes, counter-rotating and mechanically connected to swing in opposite directions was used to stabilise a bicycle. A simple mathematical model of the vehicle and a simple control algorithm have been used to develop a prototype, which was successfully tested at very low speed (up to 1 m/s). In [10], a gyroscopic stabiliser consisting of a single gyroscope spinning with respect to a vertical axis and swinging with respect to a pitch axis to stabilise the roll motion of a single track vehicle called Ecomobile has been studied. A simplified model of the dynamics of a two-wheeled vehicle that considers only the lateral position of the contact point and the roll angle was employed to develop a simple control system capable of stabilising the roll motion. The effects of steering angle, yaw motion, and tyre-road interactions are neglected and the control moment produced by the gyroscope is assumed to be directly controllable. An analog stabiliser system has been studied in [21], where a more complex model that considers curvature of the vehicle's path is used, but again the effects of steering and tyre dynamics are ignored.

The aim of this paper is to provide a general understanding of the gyroscopic stabilisation of single track vehicles by making a systematic analysis of the different aspects of the problem. Different stabiliser configurations, consisting of either one or two counter-rotating gyroscopes and swinging with respect to different axis are analysed and discussed. The influence that gyroscopic stabilisers have on capsize, weave and wobble is specifically addressed, as is the stabiliser's effect on vehicle handling.

The paper is organised as follows: first, different alternatives to generate either a roll, a yaw, or a mixed roll-yaw gyroscopic torque are illustrated first (section 2). Then, a mathematical model describing the dynamics of the combined vehicle-gyroscope system is given in Section 3. Section **??** discusses the general problem of designing the stabiliser controller and in particular the development of an optimal gain-scheduled Linear Quadratic Regulator. The system performance are then analysed both in the frequency and time domain in Section 5. Finally, results are summarised and discussed in Section 6.

2 GYROSCOPIC TORQUE GENERATION

Different configurations of gyroscopic stabilisers have been considered in the existing literature, including single gyroscopes [22, 9, 10, 21] and twin counter-rotating gyroscopes [2, 12, 11, 13], which spin either with respect to a nominal yaw [22, 10, 12, 11, 21], pitch [22, 9] and even roll [13] axis. However, the advantages and disadvantages of these different configurations are unclear, and there is no comparative analysis of their stabilisation performance. For this reason, this section introduces the principles of gyroscopic torque generation and compares all sensible configurations of one and two gyroscopes that may be used to generate a stabilising effect on a motorcycle.

The simplest way to generate a gyroscopic torque is depicted in Figure 1a and consists of a gimbal which swings by an angle σ with respect to the vertical axis z, while supporting a gyroscope with spins with constant velocity Ω with respect to the y_g axis. The gyroscope is an axially-symmetric body and its inertia tensor is a diagonal matrix $\boldsymbol{I} = diag(I_d, I_g, I_d)$, where $I_{yy} = I_g$ is the axial (spinning) inertia and $I_{xx} = I_{zz} = I_d$ are the diametral inertias. By defining $\boldsymbol{\omega}$ as the angular velocity of the gimbal and $\boldsymbol{\Omega} = (0, -\Omega, 0)^T$ as the gyroscope spinning velocity relative to the gimbal, the angular momentum of the gyroscope is:

$$\boldsymbol{K} = \boldsymbol{I}(\boldsymbol{\omega} + \boldsymbol{\Omega}) \tag{1}$$

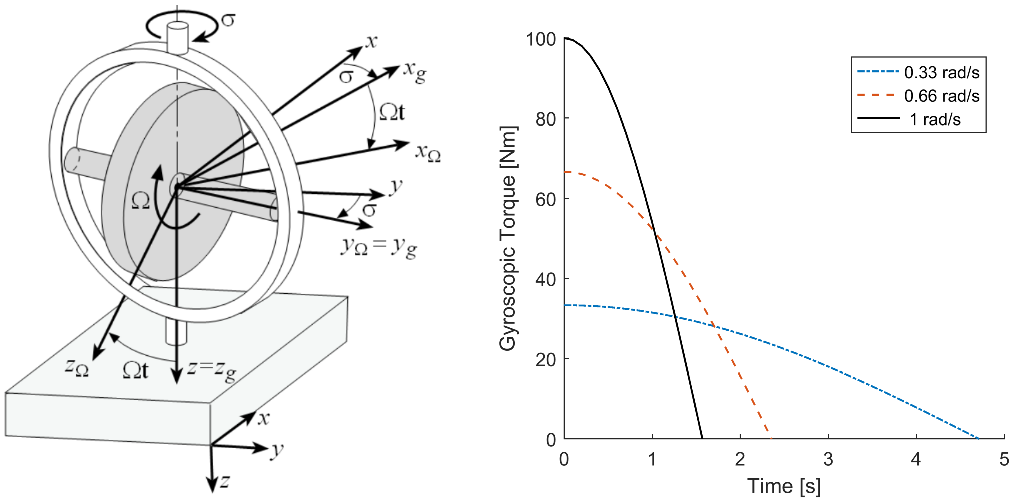

(a) The reference frame (x, y, z) is attached to the base, the frame (x_g, y_g, z_g) is attached to the swinging gimbal, and the frame $(x_\Omega, y_\Omega, z_\Omega)$ is attached to the spinning gyroscope.

(b) Gyroscopic torque G for different swinging velocities (angular momentum $I_g\Omega = 100$ Nms).

Figure 1. Gyroscopic torque generated by a gyroscope mounted on a gimbal.

Because of the axial symmetry of the gyroscope, this expression is valid both in the reference frame $(x_\Omega, y_\Omega, z_\Omega)$ attached to the gyroscope and in the reference frame (x_g, y_g, z_g) attached to the gimbal. The latter is more convenient for the derivation of Euler's equations, which read:

$$\frac{\mathrm{d}\boldsymbol{K}}{\mathrm{d}t} = \boldsymbol{I}\dot{\boldsymbol{\omega}} + \boldsymbol{\omega} \times \boldsymbol{I}(\boldsymbol{\omega} + \boldsymbol{\Omega}) = \boldsymbol{M} \tag{2}$$

where $\boldsymbol{M}$ is the moment vector of active and reactive external forces with respect to the gyroscope centre of mass and $\dot{\boldsymbol{\Omega}} = 0$ by assumption. The gyroscope torque is by definition:

$$\boldsymbol{G} = \boldsymbol{\omega} \times \boldsymbol{I\Omega} \tag{3}$$

By assuming that the spinning velocity is much greater than the angular velocity of the gimbal $\Omega \gg |\boldsymbol{\omega}|$, the term $\boldsymbol{\omega} \times \boldsymbol{I\omega}$ (which is quadratic in the angular speeds $\omega_i\omega_j$), Euler's equations may be simplified as follows:

$$\boldsymbol{I}\dot{\boldsymbol{\omega}} + \boldsymbol{G} = \boldsymbol{M} \tag{4}$$

For a fixed base, the angular velocity of the gimbal is simply $\boldsymbol{\omega} = (0, 0, \dot{\sigma})^T$ and Euler's equations become:

$$\begin{aligned} I_g\Omega\dot{\sigma} &= M_x^g \\ 0 &= M_y^g \\ I_d\,\ddot{\sigma} &= M_z^g \end{aligned} \tag{5}$$

where the suffix g highlights that vector equation (4) has been projected onto the reference frame (x_g, y_g, z_g) attached to the gimbal. In equation (5), $G = I_g\Omega\dot{\sigma}$ is the gyroscopic torque, which is orthogonal to both the spinning and swinging axes; M_y^g is the (null) torque necessary to maintain the gyroscope spin motion and M_y^g is the torque necessary to control the swing motion. The projection of the gyroscopic torque into the reference frame (x, y, z), which is attached to the base, reads:

$$\boldsymbol{G} = \begin{pmatrix} G_x \\ G_y \\ G_z \end{pmatrix} = \begin{pmatrix} I_g \Omega \, \dot{\sigma} \cos\sigma \\ I_g \Omega \, \dot{\sigma} \sin\sigma \\ 0 \end{pmatrix} \tag{6}$$

For the purpose of roll stabilisation, only the component G_x of the gyroscopic torque is useful. This torque increases with the angular speed $\dot{\sigma}$ but decreases with the angle σ. Therefore, even if a high torque can be generated by a fast swing motion, a continuous torque may be generated only for a short time (see Figure 1b). Indeed, the integral of the torque G_x for a complete swing rotation, i.e. from maximum torque ($\sigma = 0$) to null torque ($\sigma = \pi/2$), is always equal to the angular momentum of the gyroscope:

$$\int_0^T G_x \, dt = I_g \Omega \int_0^T \dot{\sigma} \cos\sigma \, dt = I_g \Omega \sin\sigma \Big|_0^{\pi/2} = I_g \Omega \tag{7}$$

Now we consider the application of a swinging gyroscope on a motorcycle which moves with angular speed $\boldsymbol{\omega}_m = (\omega_x, \omega_y, \omega_z)^T$. Consequently, the gimbal angular speed is $\boldsymbol{\omega} = (\omega_x, \omega_y, \omega_z + \dot{\sigma})^T$ in the reference frame attached to the vehicle chassis (see Figure 2a, $\alpha = 0$), while in the reference frame attached to the gimbal itself is:

$$\boldsymbol{\omega} = \begin{pmatrix} \omega_x \cos\sigma + \omega_y \sin\sigma \\ -\omega_x \sin\sigma + \omega_y \cos\sigma \\ \omega_z + \dot{\sigma} \end{pmatrix} \tag{8}$$

By introducing expression (17) into equation (3), one obtains the following expression of the roll gyroscopic torque:

$$\boldsymbol{G}_\phi = \begin{pmatrix} G_x \\ G_y \\ G_z \end{pmatrix} = \begin{pmatrix} (\omega_z + \dot{\sigma}) \cos\sigma \\ (\omega_z + \dot{\sigma}) \sin\sigma \\ -(\omega_x \cos\sigma + \omega_y \sin\sigma) \end{pmatrix} I_g \Omega \tag{9}$$

where components G_x, G_y, G_z are defined in the chassis reference frame. Equation 9 shows that the gyroscopic roll torque G_x includes not only the term generated by the swing motion $\dot{\sigma}$, but also a term in ω_z that cannot be controlled directly. Additionally, the angular velocity ω_x generates a gyroscopic moment on the z axis, so that the gyroscope creates a cross coupling between angular motion of the motorcycle about the x and z axes. There are also some coupling terms between the y and z axes. These terms are proportional to $\sin\sigma$ and therefore less significant than the previous ones.

An alternative way to generate a roll gyroscopic torque is to utilise a gyroscope which spins with respect to the yaw axis z and swings with respect to the pitch axis y (Figure 2b, assuming $\alpha = 0$). In this case the gyroscopic torque reads:

$$\boldsymbol{G}'_\phi = \begin{pmatrix} (\omega_y + \dot{\sigma}) \cos\sigma \\ \omega_z \sin\sigma - \omega_x \cos\sigma \\ -(\omega_y + \dot{\sigma}) \sin\sigma \end{pmatrix} I_g \Omega \tag{10}$$

The gyroscope now creates a pitch-roll coupling between x and y axis. This situation is quite different from the previous one: while the yaw-roll gyroscopic cross-terms (9) act in addition to the already coupled motorcycle dynamics, the roll-pitch gyroscopic cross-terms (10) create an ex-novo coupling between in-plane and out-of-plane motion, which is much less predictable and potentially more dangerous. For example, the pitch motion generated during braking, or while passing over a bump, will create a roll gyroscopic torque which may capsize the vehicle. For this reason, we believe that this configuration is unsuitable for stabilising purposes and will not be considered further in this paper.

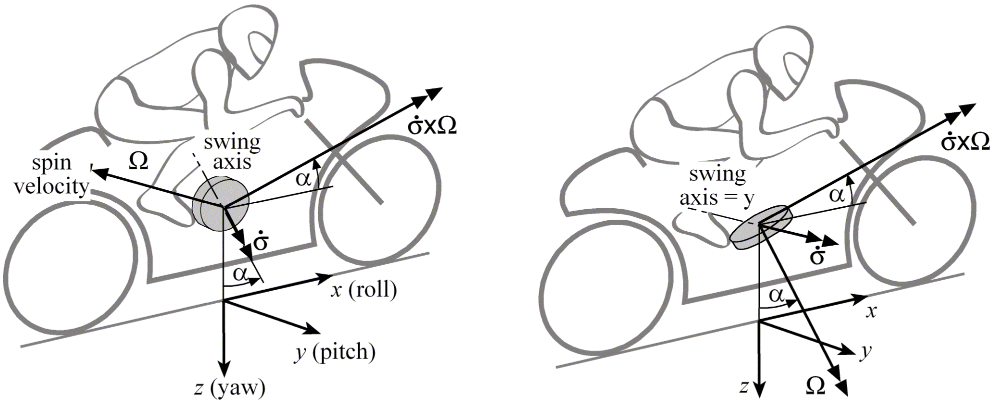

(a) Gyroscope spinning with respect to the y axis, gimbal swinging with respect to an axis in the xy plane.

(b) Gyroscope spinning with respect to an axis in the xy plane, gimbal swinging with respect to the y axis.

Figure 2. Equivalent layouts that generate the same gyroscopic torque.

However, for both the pitch-spinning and yaw-spinning configurations, it is possible to almost cancel the cross-coupling effects by using a pair of counter-rotating gyroscopes. More precisely, by using two equal gyroscopes $I_{g1} = I_{g2} = I_g/2$ with opposite spin and swing rotations $\Omega_{1,2} = \pm\Omega$, $\sigma_{1,2} = \pm\sigma$, the expression of the gyroscopic torques (9) and (10) both reduce to:

$$\boldsymbol{G}''_\phi = \begin{pmatrix} \dot{\sigma}\cos\sigma \\ \omega_z \sin\sigma \\ -\omega_y \sin\sigma \end{pmatrix} I_g\Omega \tag{11}$$

The cross coupling between x and z axes has been completely eliminated and the roll torque depends on the swing motion only. G_z still depends on the pitching angular rate, but for small swing angles this term is small too.

Motorcycle stability is not only related to the roll motion, for example weave stability is heavily associated to the yaw motion. Therefore, a yaw gyroscopic torque may be in principle used to improve stability. A yaw gyroscopic torque may be generated by using a gyroscope which spins with respect to the pitch axis y and swings with respect to the roll axis x (Figure 2a, assuming $\alpha = \pi/2$). The complete expression of the gyroscopic torque is:

$$\boldsymbol{G}_\psi = \begin{pmatrix} \omega_z\cos\sigma - \omega_y\sin\sigma \\ (\omega_x + \dot{\sigma})\sin\sigma \\ -(\omega_x + \dot{\sigma})\cos\sigma \end{pmatrix} I_g\Omega \tag{12}$$

Alternatively a gyroscope which spins with respect to the roll axis x and swings with respect to the pitch axis y may be used (Figure 2a, assuming $\alpha = Pi/2$), the corresponding gyroscopic effect is:

$$\boldsymbol{G}'_\psi = \begin{pmatrix} -(\omega_x + \dot{\sigma})\sin\sigma \\ (\omega_x\sin\sigma + \omega_z\cos\sigma) \\ -(\omega_x + \dot{\sigma})\cos\sigma \end{pmatrix} I_g\Omega \tag{13}$$

The gyroscopic torques (12) and (13) contain not only the swing gyroscopic term $I_g\Omega\dot{\sigma}$, which is generated purposefully and may be controlled, but also some additional cross-coupling terms which cannot be controlled directly. For the pitch-spinning gyroscope (12), the main cross-coupling is between the yaw and roll motion (with a minor coupling between pitch and yaw), while for the the roll-spinning gyroscope (13), the main cross-coupling is between the yaw and pitch motion (plus a minor coupling between roll and yaw). As discussed for the roll torque case, the gyroscopic coupling between between in-plane and out-of-plane motion has to be avoided because it is highly unpredictable and potentially dangerous, so the second configuration will not be considered further.

Once again, the utilisation of two equal counter-rotating and counter-swinging gyroscopes makes it possible to cancel the main cross-coupling terms, and the gyroscopic torque becomes:

$$\boldsymbol{G}''_{\psi} = \begin{pmatrix} -\omega_y \sin\sigma \\ \omega_x \sin\sigma \\ -\dot{\sigma}\cos\sigma \end{pmatrix} I_g \Omega \tag{14}$$

an expression which is valid for both the x- and y-axis spinning layouts.

It is useful to generalise the results discuss above to consider the generation of a gyroscopic torque which has both roll and yaw components. For a couple of pitch-spinning gyroscopes swinging by an axis inclined by the angle α with respect to the yaw axis (Figure 2a), the gyroscopic torque on the chassis may be calculated as follows:

$$\boldsymbol{G} = \boldsymbol{G}_{\phi}\cos\alpha + \boldsymbol{G}_{\psi}\sin\alpha \tag{15a}$$

$$\boldsymbol{G} = \begin{pmatrix} \dot{\sigma}\cos\sigma\cos\alpha - \omega_y \sin\sigma\sin\alpha \\ (\omega_x \sin\alpha + \omega_z\cos\alpha)\sin\sigma \\ -(\omega_y\sin\sigma\cos\alpha + \dot{\sigma}\cos\sigma\sin\alpha) \end{pmatrix} I_g\Omega + \frac{i_1+i_2}{2} \begin{pmatrix} \omega_z\cos\sigma \\ \dot{\sigma}\sin\sigma \\ -\omega_x\cos\sigma \end{pmatrix} I_g\Omega \tag{15b}$$

where i_1, i_2 indicates the spinning and swinging directions of the gyroscopes. In other words $i_{1,2} = 1$ represents the single gyroscope configuration, while $i_{1,2} = \pm 1$ represents the twin counter-rotating gyroscope configuration. In the latter case, the equation remains valid also in the case of gimbals swinging with respect to the pitch axis and gyroscopes spinning with respect to an axis inclined by the angle α with respect to the yaw axis, see Figure 2b.

3 DYNAMICS OF THE SINGLE TRACK VEHICLE WITH GYROSCOPES

This section summarises the mathematical model to be used for analysing the influence of the gyroscopic system on vehicle stability. The proposed model is based on the seminal work on the dynamics of motorcycles [20], which derives a mathematical model of the dynamics of the motorcycle using Lagrangian mechanics and investigates the stability properties when the vehicle is moving with a given velocity by linearising the system and calculating the eigenvalues of the state-space matrices. This is the simplest model which is capable of capturing the behaviour of the weave, wobble and capsize with good accuracy. The model proposed here includes five rigid bodies (front chassis, rear chassis, rider, and the two wheels, see Figure 3)) and has five degrees of freedom: roll ϕ, yaw ψ, and steer δ angles, plus longitudinal velocity u, and lateral velocity v. The main differences with the Sharp model consist of a more accurate description of tyre behavior, considering a variable longitudinal speed and, of course, the inclusion of the gyroscopic stabiliser.

The equations of motion are derived by using Newtonian mechanics with the assistance of the Maple-based toolbox MBSymba [15, 17], which is used to derive the equations of motion that are then linearised with respect to a straight running configuration, that corresponds to zero roll ϕ, yaw ψ, pitch μ, and steer δ angles, as well as their derivatives, and zero lateral velocity v.

The full set of equations and the details of their derivation are given in [16], while here we just focus on the differences between a traditional single-track vehicle and one equipped with an actively controlled gyroscope. For the motorcycle as a whole system, we can write three scalar equations

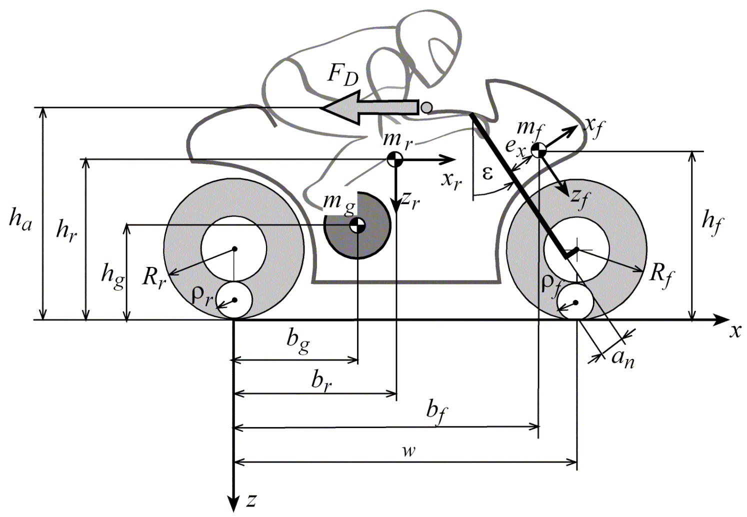

Figure 3. Motorcycle geometry

Table 1. Motorcycle parameters

parameters	value		description
w	1.413	m	wheelbase
e	0.0408	m	eccentricity
ε	21.2	$^\circ$	castor angle
a_n	0.112	m	mechanical trail
c_δ	6	$Nm/rad\ s^{-1}$	steering column damping
$C_D A$	0.35	m^2	drag coefficient
m_f, m_r	39, 216.2	kg	front and rear chassis mass
(b_f, h_f)	(1.38, 0.506)	m	x-y position of front centre of mass
(b_r, h_r)	(0.522, 0.538)	m	x-y position of rear centre of mass
$I_{fxx}, I_{fyy}, I_{fzz}$	4.57, 4.72, 0.781	kgm^2	front principle moments of inertia
$I_{rxx}, I_{ryy}, I_{rzz}$	12.4, 32.1, 27.2	kgm^2	rear principle moments of inertia
R_f, R_r	0.319, 0.3	m	front and rear tyre radius
ρ_f, ρ_r	0.06, 0.105	m	tyre cross-sectional radius of curvature
σ_f, σ_r	0.165, 0.21	m	front and rear relaxation length
$C_{f\lambda}$, $C_{f\phi}$	9.68, 0.91	–	front tyre stiffnesses
$C_{r\lambda}$, $C_{r\phi}$	13.7, 1.20	–	rear tyre stiffnesses
C_{fa}, C_{ra}	0.407, 0.383	–	self-aligning moment coefficients
C_{ft}, C_{rt}	0.023, 0.023	–	overturning moment coefficients
I_g	0.0318	kgm^2	axial moment of inertia
I_d	0.0175	kgm^2	diametral moment of inertia
m_g	10	kg	gyroscope mass
(b_g, h_g)	(0.6, 0.7)	m	x-y position of centre of mass
Ω	30000	RPM	spinning angular velocity

for the translational motion and another three for the rotational motion. The translational equations are not affected by the addition of the gyroscopic stabiliser, while the rotation equations read

$$\boldsymbol{I}_0\dot{\boldsymbol{\omega}} + \boldsymbol{G}_0 + \boldsymbol{G} = \boldsymbol{M}_0 \tag{16}$$

where the terms with the suffix 0 are related to a standard motorcycle, while $\boldsymbol{G}$ is the additional term due to the gyroscopic stabiliser. The latter may be determined according to the expressions derived in Section 2, which in turn requires the calculation of vehicle angular velocity in terms of the yaw, roll and pitch angles

$$\boldsymbol{\omega} = \begin{pmatrix} \omega_x \\ \omega_y \\ \omega_z \end{pmatrix} = \begin{pmatrix} \cos(\mu)\,\dot{\phi} - \sin(\mu)\cos(\phi)\,\dot{\psi} \\ \sin(\phi)\,\dot{\psi} + \dot{\mu} \\ \sin(\mu)\,\dot{\phi} + \cos(\mu)\cos(\phi)\,\dot{\psi} \end{pmatrix} \simeq \begin{pmatrix} \dot{\phi} \\ \dot{\mu} \\ \dot{\psi} \end{pmatrix} \tag{17}$$

By substituting angular velocity (17) into equation (15) and then neglecting all small terms which are quadratic in the angular velocities, we obtain the following linearised expression for the gyroscopic torque:

$$\boldsymbol{G} = \begin{pmatrix} \dot{\sigma}\cos\alpha + \frac{i_1+i_2}{2}\dot{\psi} \\ 0 \\ -\dot{\sigma}\sin\alpha - \frac{i_1+i_2}{2}\dot{\phi} \end{pmatrix} I_g\Omega \tag{18}$$

It is worth emphasising that in the linearised expression for the gyroscopic torque (18) there are no longer any coupling terms between in-plane pitch motion and out of plane yaw/roll motion, hence it is not necessary to consider the vehicle pitch associated with movement of the suspension.

To complete the set of motorcycle equations, we need to add the steering equation of motion, which is not affected by the gyroscopic stabiliser, as well as relaxation equations for tyres.

Finally, we must consider the gyroscope swinging equation of motion, which reads

$$I_d\ddot{\sigma} + \tfrac{i_1+i_2}{2} I_d \left(\ddot{\phi}\sin\alpha + \ddot{\psi}\cos\alpha\right) = T_\sigma + \left(\dot{\phi}\cos\alpha - \dot{\psi}\sin\alpha\right) I_g\Omega \tag{19}$$

where T_σ is the torque that will be used for the active control of the swing motion.Equation (19) is valid for the twin gyroscope system too, provided that the two gyroscopes are mechanically constrained to swing by equal angles in opposite directions.

After reducing the second order differential equations to the first order, the linearised equations of motion of the whole system may be expressed as a state space system:

$$\mathbf{E}\dot{\boldsymbol{x}} = \mathbf{A}(t)\boldsymbol{x} + \mathbf{B}\boldsymbol{u} \tag{20}$$

which includes three additional velocity variables, respectively $\dot{\phi} = \omega_\phi$, $\dot{\delta} = \omega_\delta$, and $\dot{\sigma} = \omega_\sigma$. Matrix $\mathbf{E}$ is constant and symmetric, while $\mathbf{A}(t)$ depends on time due to the effect of the longitudinal velocity u and acceleration $\dot{u} = a_x$. The state $\boldsymbol{x}$ is a 10-dimensional vector

$$\boldsymbol{x} = (v, \omega_\psi, \omega_\phi, \omega_\delta, Y_r, Y_f, \phi, \delta, \omega_\sigma, \sigma)^T \tag{21}$$

The input vector is made up of two variables

$$\boldsymbol{u} = (T_\delta, T_\sigma)^T \tag{22}$$

namely the rider steering torque T_δ and gyroscope(s) swinging torque T_σ. Analytical expressions for the matrices $\mathbf{E}$, $\mathbf{A}$ and $\mathbf{B}$ are given in [16]

Table 2. Setpoints for gain-scheduled controllers

u_i	q_i	r_i
80	10^6	1
16	10^6	1
4	1	10^{-3}
0.5	1	10^{-3}

4 ACTIVE GYROSCOPIC STABILISATION

In this section we discuss the possibility of using an active system that controls the swing motion of the gyroscope(s) to further improve vehicle stability.

As the principal objective is to understand the potential of gyroscopic stabilisers, we consider the design of a full-state feedback controller, where the torque applied to the gyroscope is a linear function of the current state vector:

$$T_\sigma = -\boldsymbol{K}\boldsymbol{x} \tag{23}$$

The matrix $\boldsymbol{K}$ is chosen to correspond to the infinite-horizon linear quadratic regulator (LQR) for the cost function

$$J = \int_0^\infty \left(\phi^2 + q\sigma^2 + rT_\sigma^2\right) dt \tag{24}$$

where q is a tuning parameter that penalises the swing angle, and r denotes a tuning parameter that penalises swing input torque. This has the advantage that one may compare different system configurations (such as using a single or twin gyroscope, or different orientations) in a straightforward and unified way by retaining the same cost function for each case.

Since system eigenvalues vary with the speed and longitudinal acceleration, a constant set of gains $\boldsymbol{K}$ is not capable of stabilising the vehicle in the whole range of operating conditions. To solve this problem, feedback gains are linearly interpolated between gain-scheduled controllers defined by a feedback matrix K_i and a speed setpoint u_i, which are given in Table 2 together with the corresponding cost function weights. At the low speed setpoints (0.5 m/s and 4 m/s) an equal penalty has been given to both the swing and roll angle, with an input penalty present in order to stabilise the system using as little swing torque as possible. At higher speeds (the 16 m/s and 80 m/s setpoints) any swing motion is heavily penalised instead. In this way the gyroscope motion is constrained by the controller and the motorcycle has similar high-speed dynamics to when the gyroscope is not present.

5 PERFORMANCE ANALYSIS

The result of applying this controller to the system is shown in Figure 4 in terms of the root loci of the controlled system.

Figure 4a shows the eigenvalues of the motorcycle with active gyroscopic stabilisation (but without rider control, $T_\delta = 0$) for a speed varying from 0.5 m/s and 80 m/s. Low speed capsize and weave have been now stabilised, see Figure 4b. This low speed stabilisation is not very robust, and gain scheduling should be employed appropriately. Because the vehicle rollover stabilisation is particularly important during braking, this situation has been analysed too. In [19] and [8], it is shown that the time-varying linear system (20) is stable when the associated frozen-time eigenvalues are negative, and the rate of change of $\boldsymbol{A}(t)$ is sufficiently slow. Therefore, eigenvalue analysis is used here to assess braking stability as is also done, for example, in [14, 5, 6]. Without changing the control gains, the beneficial effect of this active stabilisation is clearly visible in the whole speed range, as visible in Figure 5a-b.

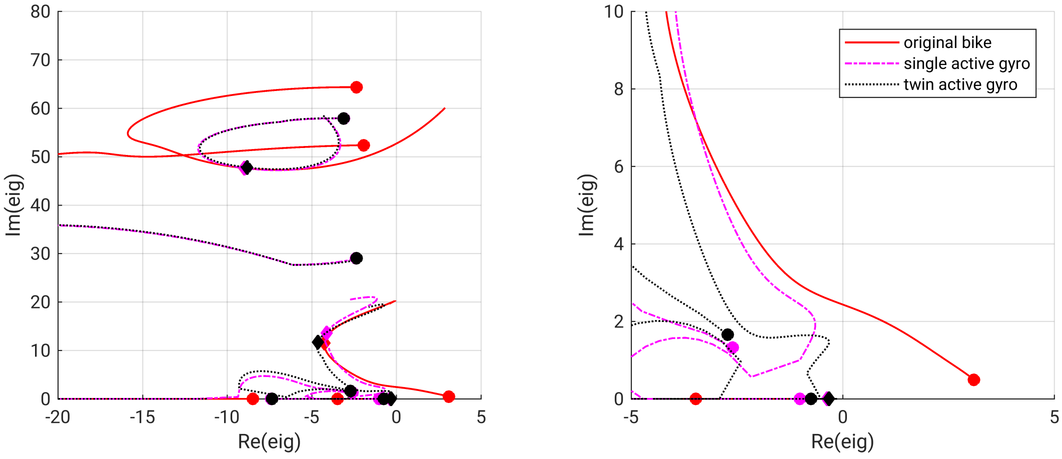

(a) Root loci (overview) (b) Root loci (zoom)

Figure 4. Root loci, constant speed motion (different speed between 0.5 and 80 m/s).

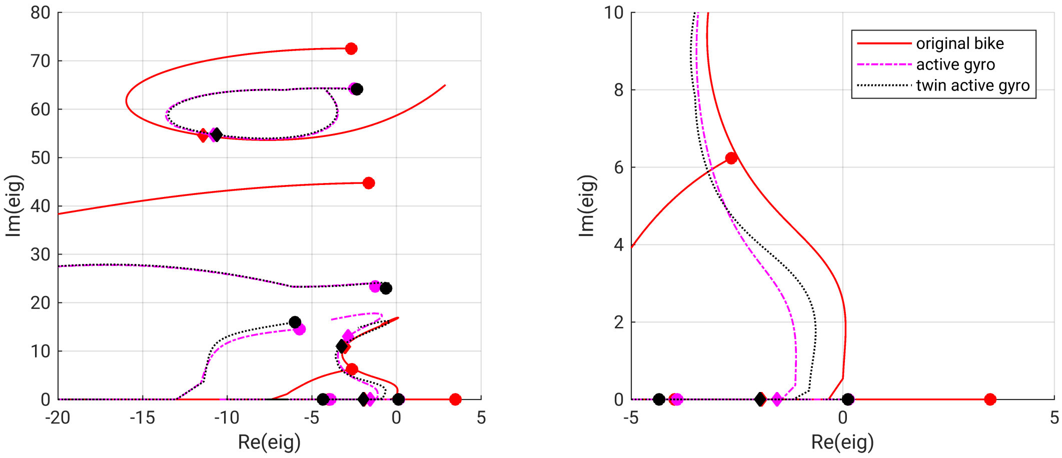

(a) Root loci (overview) (b) Root loci (zoom)

Figure 5. Root loci, braking with constant deceleration 4 m/s^2 (speed between 0.5 and 80 m/s).

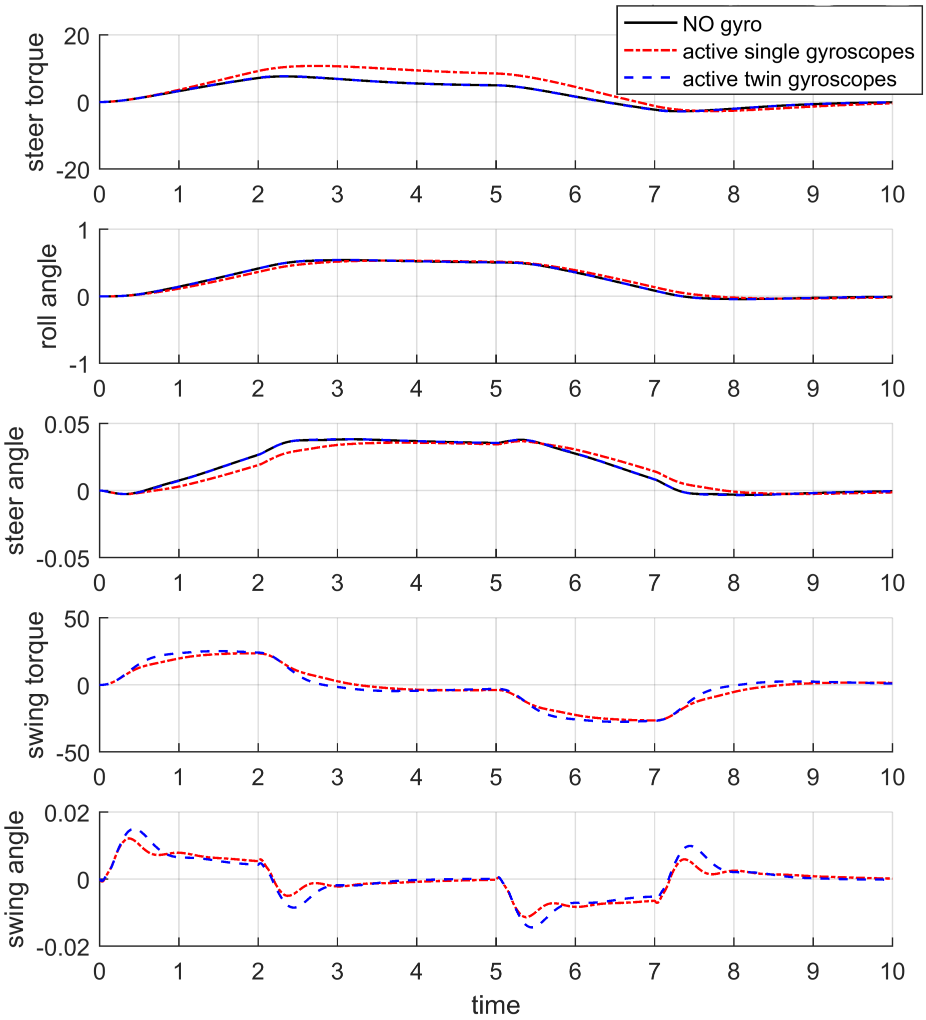

Figure 6. Motorcycle response under cornering (active gyroscopic stabiliser, speed 15 m/s).

It is also essential to verify that the stabilised motorcycle has acceptable cornering performance. Figure 6 gives the response of the gyroscope during cornering manoeuvres at speed of 15 m/s, when the active gyroscopic stabiliser cooperates with the rider.With a twin gyroscope stabiliser, the cornering response in term of steer torque and roll angle is practically identical to that of the original vehicle. With a single gyroscope, a higher steering torque is required and the roll angle response is slightly delayed. In both cases, the gyroscopic swing torque has a peak value of approximately 25 Nm. Noting that in both cases the peak value of gyroscope swing rate is around 0.1 rad/s, we conclude that the gyroscope actuation draws a peak power of approximately 2.5 W.

The dynamic behavior of the motorcycle may be furthered discussed by inspecting frequency response functions (FRFs). The vehicle now has two separate, independent inputs: the steer torque, which is controlled by the rider, and the gyroscope swing torque given by the active controller. Figure 7a shows the magnitude of the steer torque to roll angle FRF, calculated when the gyroscope control loop is closed. When using a single gyroscope, the DC gain of this transfer function is reduced, corresponding to the increased steer torque required in the cornering simulation when using only a single gyroscope. At a frequency of 1 Hz and above, the magnitude response between the original vehicle and the stabilised one is practically the same, therefore the influence of the stabiliser in fast transient manoeuvres will be negligible. The figure also shows that the adoption of

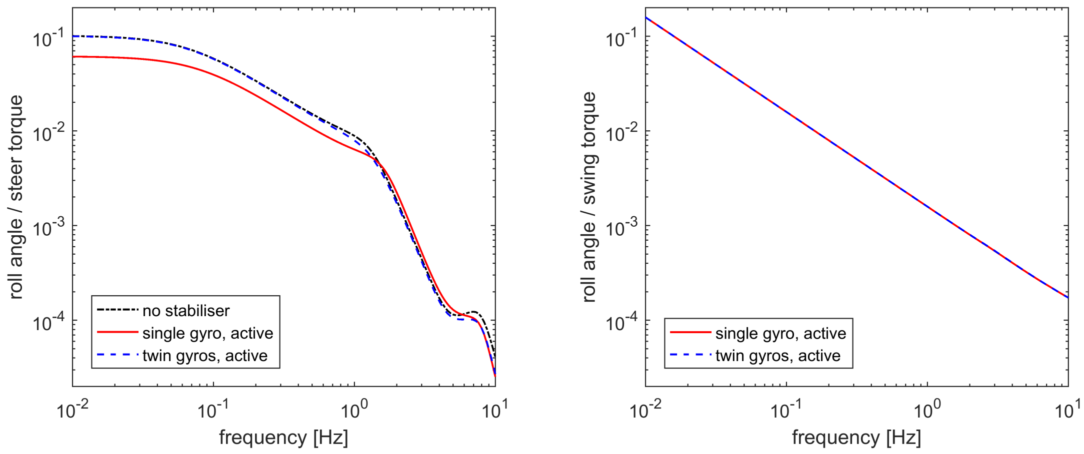

(a) roll torque to steer angle

(b) swing torque to steer angle

Figure 7. Magnitude of frequency response functions (speed 15 m/s).

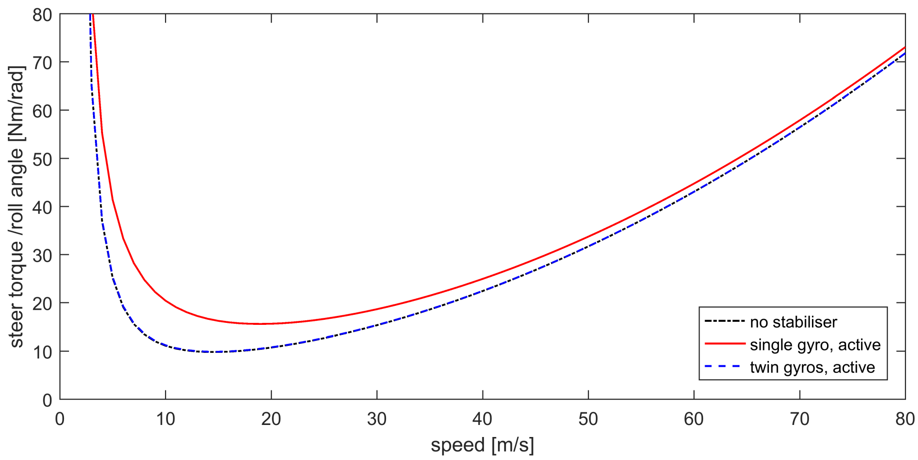

Figure 8. Steering torque to roll angle ratio in steady cornering.

twin counter-rotating gyroscopes makes it possible to approximately maintain the original vehicle handling characteristics. Figure 7b shows the magnitude of the swing torque to roll angle FRF, calculated without any rider control action or steering torque (hands-off). This transfer function approximates an integrator at the low to medium frequencies, shown. Moreover it includes a small resonance peak at high frequencies (although this is well above the range of interest for handling). At very low-frequency, the magnitude of the swing-to-roll FRF is greater than the magnitude of the steer-to-roll FRF, suggesting that the gyroscope may be more effective than the handlebars to control the vehicle roll in static conditions. However, this is not actually true because the gyroscope swing angle is constrained to remain small. As a consequence, the feedback controller must attenuate low frequencies and cannot be used to reach a static roll angle setpoint rather than the equilibrium one. As far as speed is concerned, the variations of the steer torque to roll angle response function that occurs for the reference motorcycle are replicated for both the single and twin gyroscopes. Moreover, the swing torque to roll angle response function is insensitive to the speed. This is not surprising, as the swing torque induces a gyroscopic effect which is applied directly on the chassis, while by contrast the steer torque to roll angle control is enforced trough tyre lateral forces, which depend on speed.

So far, the twin gyroscope configuration appears to be more suitable to preserve the original vehicle handling characteristics than the single gyroscope configuration. To further investigate this matter, figure 8 reports the steer torque to roll angle ratio (i.e. the reciprocal of the static of figure 7a) as a function of the speed. As already reported in [3], it may be observed that it is quite difficult to control the motorcycle at very low speed, and then the steering torque effort has a minimum at a relatively low speed and increases again with the speed. Even if the single gyroscopic stabiliser is not able to match perfectly this behavior as the twin gyroscopic stabiliser does, the increase in steering torque required in steady cornering is modest if the whole range of speed is considered. Indeed, the angular momentum of the gyroscope is constant and, as the speed increases, the angular momentum of the front wheel becomes dominant instead [4, 7].

6 CONCLUSIONS

The paper has explored the potential of gyroscopic systems for the stabilisation of the weave, wobble and capsize modes of motorcycles and single track vehicles more generally. First, different gyroscope configurations were examined, including different orientations of both the spinning and swinging (precessing) axes, and for both single and twin counter-rotating gyroscopes. It has been shown that the most sensible configurations that should be used to stabilise a motorcycle are either a single gyroscope spinning with respect to an axis parallel to the wheel spin axis and swing with respect to the yaw axis, or a system of twin gyroscopes counter-rotating and counter-swinging with respect to the same axes. It has been also shown that the latter and a system composed by twin gyroscopes counter-spinning with respect to the yaw axis and counter-swinging with respect to the pitch axis are completely equivalent. Any other configuration presented serious disadvantages.

Active stabilisation systems, that is when the gyroscope motion is feedback controlled, have shown greater performance and in particular are capable of stabilising the motorcycle at almost zero speed and during braking. This characteristic could be very useful to improve driving comfort, for example by allowing the rider to avoid putting their feet down when riding very slowly or stopping at intersections, as well as being benificial for safety, e.g. in combination with an emergency braking system to avoid - or at least mitigate - collisions. While we did not find a significant difference between a single active gyroscope and a twin counter-rotating gyroscope system in term of vehicle stabilisation, the latter performs better than the former in terms of handling. Indeed a twin gyroscopic system may have practically no effect on the handling characteristics of the original vehicle. However, the handling differences for the single gyroscope case are appreciable only in the medium speed range and, considering the greater complexity of the twin gyroscopes versus the single one, it is not clear which of the two cases presents the more attractive option. In term of control system, gain-scheduling LQR controllers seem to provide an effective control methodology. However, this assumes that the full state is available for feedback and so future work should consider output feedback strategies (for instance, using a state observer). The non-linearities associated with both vehicle roll and gyroscope swing angle also require further investigation, as well as the sensitivity of the stabilisation to speed and acceleration changes (e.g. by considering parameter-dependent Lyapunov functions, as is common in the LPV systems literature).

REFERENCES

[1] BENZ, C. Self-propelling vehicle. 385087, 1888.

[2] BEZNOS, A., FORMAL'SKY, A., GURFINKEL, E., JICHAREV, D., LENSKY, A., SAVITSKY, K., AND TCHESALIN, L. Control of autonomous motion of two-wheel bicycle with gyroscopic stabilization. vol. 3, pp. 2670–2675.

[3] BIRAL, F., BORTOLUZZI, D., COSSALTER, V., AND DA LIO, M. Experimental study of motorcycle transfer functions for evaluating handling. Vehicle System Dynamics 39, 1 (2003), 1–25.

[4] COSSALTER, V., DORIA, A., AND LOT, R. Steady turning of two-wheeled vehicles. Vehicle System Dynamics 31, 3 (1999), 157–181.

[5] COSSALTER, V., LOT, R., AND MAGGIO, F. The modal analysis of a motorcycle in straight running and on a curve. Meccanica 39, 1 (2004), 1–16.

[6] COSSALTER, V., LOT, R., AND MASSARO, M. An advanced multibody code for handling and stability analysis of motorcycles. Meccanica 46, 5 (2011), 943–958.

[7] COSSALTER, V., LOT, R., AND PERETTO, M. Steady turning of motorcycles. Proceedings of the Institution of Mechanical Engineers, Part D: Journal of Automobile Engineering 221, 11 (2007), 1343–1356.

[8] DESOER, C. Slowly varying system x = a(t)x. IEEE Transactions on Automatic Control 14, 6 (1969), 780–781.

[9] HAIR, J. M. Gyro stabilized remote controlled toy motorcycle. Patent US 5820439, 1998.

[10] KARNOPP, D. Tilt control for gyro-stabilized two-wheeled vehicles. Vehicle System Dynamics 37, 2 (2002), 145–156.

[11] KIM, D. K. Y. Dynamically balanced flywheel. Patent US 2013/0233100 Al, 2013.

[12] KIM, D. K. Y., AND BRETNEY, K. Electrical system for gyroscopic stabilized vehicle. Patent US 2011/0231041 A1, 2011.

[13] KLEWS, M. Method and device for the driving stabilization of a motorized two-wheeled vehicle using a double-gyroscope device. Patent US 2015/0353151 Al, 2015.

[14] LIMEBEER, D., EVANGELOU, S., AND SHARP, R. Stability of motorcycles under acceleration and braking. vol. 6 C, pp. 2583–2591.

[15] LOT, R., AND DA LIO, M. A symbolic approach for automatic generation of the equations of motion of multibody systems. Multibody System Dynamics 12, 2 (2004), 147–172.

[16] LOT, R., AND FLEMING, J. Gyroscopic stabilisers for powered two-wheeled vehicles. Vehicle System Dynamics 57, 9 (2019), 1381–1406.

[17] LOT, R., AND MASSARO, M. A symbolic approach to the multi-body modelling of road vehicles. International Journal of Applied Mechanics (2017, in printing).

[18] MARUMO, Y., AND NAGAI, M. Steering control of motorcycles using steer-by-wire system. User Modeling and User-Adapted Interaction 45, 5 (2007), 445–458.

[19] ROSENBROOK, H. The stability of linear time-dependent control systems. Journal of Electronics and Control 15, 1 (1963), 73–80.

[20] SHARP, R. S. The stability and control of motorcycles. Journal of mechanical engineering science 13, 5 (1971), 316–329.

[21] SPRY, S. C., AND GIRARD, A. R. Gyroscopic stabilisation of unstable vehicles: configurations, dynamics, and control. Vehicle System Dynamics 46, S1 (2008), 247–260.

[22] SUMMER, T. O. Gyro stabilized vehicle. Patent US 3410357, 1968.